Fermi-Fermi mixtures in the strong-attraction limit

M. Iskin and C. A. R. Sá de Melo
School of Physics, Georgia Institute of Technology, Atlanta, Georgia 30332-0432, USA
and Joint Quantum Institute, National Institute of Standards and Technology and University of Maryland, Gaithersburg, Maryland 20899-8423, USA
(Received 27 September 2007; published 31 January 2008)

The phase diagrams of low density Fermi-Fermi mixtures with equal or unequal masses and equal or unequal populations are described at zero and finite temperatures in the strong attraction limit. In this limit, the Fermi-Fermi mixture can be described by a weakly interacting Bose-Fermi mixture, where the bosons correspond to Feshbach molecules and the fermions correspond to excess atoms. First, we discuss the three and four fermion scattering processes, and use the exact boson-fermion and boson-boson scattering lengths to generate the phase diagrams in terms of the underlying fermion-fermion scattering length. In three dimensions, in addition to the normal and uniform superfluid phases, we find two stable nonuniform states corresponding to (i) phase separation between pure unpaired (excess) and pure paired fermions (molecular bosons); and (ii) phase separation between pure excess fermions and a mixture of excess fermions and molecular bosons. Lastly, we also discuss the effects of the trapping potential in the density profiles of condensed and noncondensed molecular bosons, and excess fermions at zero and finite temperatures, and discuss possible implications of our findings to experiments involving mixtures of ultracold fermions.

DOI: 10.1103/PhysRevA.77.013625 PACS number(s): 03.75.Ss, 03.75.Hh, 05.30.Fk

I. INTRODUCTION

The lack of precise control over standard condensed matter systems has hindered the development of experiments that can probe systematically the effects of strong correlations. However, the large degree of control in atomic systems has made them powerful tools for studying many condensed matter phenomena, and in particular superfluid phases [1–6]. For instance, a current research frontier is the study of fermion mixtures with population imbalance [7–10]. Since the population of each component as well as their interaction strength are experimentally tunable, these knobs enabled the study of the Bardeen-Cooper-Schrieffer (BCS) to Bose-Einstein condensation (BEC) evolution in population imbalanced two-component fermion superfluids [7–10]. In contrast with the crossover physics found in the population balanced case [11–13], these experiments have demonstrated the existence of phase transitions between normal and superfluid phases, as well as phase separation between superfluid (paired) and normal (excess) fermions as a function of population imbalance [14–20].

Motivated by these recent experiments, there has been intense theoretical interest in understanding the phase diagram of population imbalanced mixtures [21–29]. So far, an accurate description of such mixtures is only available in the weak fermion attraction limit, and it is yet to be developed for intermediate fermion attraction around unitarity, or for the strong attraction limit. Some progress has been made in the strong attraction limit, where Fermi-Fermi mixtures were described as a weakly interacting Bose-Fermi mixture [22,26,30,31], however, except for Ref. [22], the effective boson-fermion and boson-boson scattering parameters were obtained only in the Born approximation. In Ref. [22], it was discussed that a diagrammatic approach beyond the Born approximation is necessary to calculate exact scattering lengths and to obtain density profiles.

Strictly speaking, the Bose-Fermi description is valid only in the strong attraction limit, but may also provide semiquantitative understanding of the phase diagram close to unitarity. Thus, the main goal of this manuscript is to analyze the boson-fermion and boson-boson scattering parameters beyond the Born approximation for arbitrary mass ratio of fermions, and use the effective Bose-Fermi mixture description to generate improved phase diagrams and density profiles of Fermi-Fermi mixtures with equal or unequal masses in the strong attraction limit beyond the Born and mean-field approximations [26,30,32–34].

The main results of this manuscript are as follows. First, we analyze three- and four-fermion scattering processes and obtain the exact boson-fermion and boson-boson scattering lengths as a function of mass anisotropy. Second, we use the exact boson-fermion and boson-boson scattering parameters to construct the phase diagram for Fermi-Fermi mixtures in the strong attraction limit. In addition to the normal (N) and uniform superfluid (U) phases, we find two different nonuniform phase-separated (PS) states: (i) PS(1) with phase separation between pure unpaired (excess) and pure paired fermions (molecular bosons), and (ii) PS(2) with phase separation between pure excess fermions and a mixture of excess fermions and molecular bosons, depending on the fermion-fermion scattering parameter. The phase boundaries are very sensitive to the masses of the fermions, and also to the boson-fermion and boson-boson interactions. For equal mass mixtures, our results for the phase boundary between the PS(2) and the uniform (U) phase improves on previous saddle-point (mean-field) results, and the quantitative changes are substantial, but not dramatic. However, there is a dramatic increase in quantitative differences between mean-field and the present results for unequal mass mixtures as the mass ratio deviates from one. In particular, these differences are more pronounced when heavier fermions are in excess indicating the importance of taking into account scattering

processes beyond the Born approximation. Furthermore, we discuss the effects of the trapping potential on the density profiles of condensed and noncondensed molecular bosons, as well as excess fermions at zero and finite temperatures. Lastly, we discuss the implications of our findings to possible experiments involving Fermi-Fermi mixtures with equal or unequal masses and equal or unequal populations.

The remainder of this manuscript is organized as follows. In Sec. II, we discuss briefly the Hamiltonian for Fermi-Fermi mixtures with equal or unequal masses and emphasize that the system reduces effectively to a Bose-Fermi mixture of molecular bosons and excess fermions in the strong attraction limit. In Sec. III, we analyze the exact boson-fermion and boson-boson scattering lengths as a function of mass anisotropy, which are used to calculate the resulting phase diagram of Fermi-Fermi mixtures in the strong attraction limit. In Sec. IV, we discuss the stability of the effective Bose-Fermi mixture of molecular bosons and excess fermions in three, two, and one dimensions. We analyze the stability of population imbalanced Fermi-Fermi mixtures in the strong attraction limit in Sec. IV B, and we construct the phase diagrams of these systems in Sec. IV C. In Sec. V, we discuss the effects of harmonic traps on the density profiles of condensed and noncondensed molecular bosons, and excess fermions at zero and finite temperatures, and show their experimental signatures. Lastly, we present a summary of our conclusions in Sec. VI.

II. HAMILTONIAN

In order to calculate the correct phase diagrams of Fermi-Fermi mixtures in the strong attraction limit, it is necessary to obtain first the correct scattering parameters between two Bose molecules (paired fermions), and also between a Bose molecule and an unpaired fermion. To achieve this task, we begin by describing the Hamiltonian density for a mixture of fermions (in units of $\hbar = k_B = 1$) as

$$H(x) = \sum_{\sigma} \bar{\psi}_{\sigma}(x) \left[-\frac{\nabla^2}{2m_{\sigma}} - \mu_{\sigma} \right] \psi_{\sigma} - g \bar{\psi}_{\uparrow}(x) \bar{\psi}_{\downarrow}(x) \psi_{\downarrow}(x) \psi_{\uparrow}(x), \tag{1}$$

where $\bar{\psi}_{\sigma}(x)$ is the field corresponding to the creation of a fermion with pseudospin index σ, at position and time $x \equiv (\mathbf{r}, \tau)$. Here, $g > 0$ is the strength of the attractive fermion-fermion interaction and σ identifies two types of ($\uparrow$ and $\downarrow$) fermions. This notation allows the analysis of a mixture of fermions with equal or unequal masses, as well as equal or unequal chemical potentials. Throughout the manuscript, we assume that the lighter fermions are always $\uparrow$ and that the heavier fermions are always $\downarrow$, as intuitively suggested by the direction of the arrows, and that the chemical potentials μ_{σ} fix the population (density) n_{σ} of each type of fermion independently.

The contact interaction Hamiltonian given in Eq. (1) generalizes the equal mass and equal chemical potential Hamiltonian that is used to study the BCS to BEC evolution within the functional integral formalism [13]. The functional integral formulation [13,26,30,31] captures some essential features of the evolution from BCS to BEC superfluidity for Fermi mixtures with equal or unequal masses as well as with equal or unequal populations. However, truly quantitative results are currently possible only in the BCS limit, where the theory is simple, but the temperatures required to reach the BCS regime are very low and difficult to be achieved experimentally. In the unitarity regime, experiments can be performed and the phase diagram can be explored since the critical temperature for superfluidity is attainable, but an accurate theoretical description of this regime is still lacking. While in the BEC limit, not only the temperature required to reach the BEC regime is experimentally achievable, but also the theory becomes simple since the Fermi-Fermi mixtures can be described effectively by a weakly interacting mixture of molecular bosons and excess fermions [22,26,30,31]. However, our initial proposals of such effective Bose-Fermi mixtures [26] can provide only semiquantitative results for comparison with experiments in the BEC regime since the scattering parameters for two molecular bosons and a molecular boson and an excess fermion are obtained only in the Born approximation. In order to overcome this deficiency, we discuss next the boson-fermion and boson-boson scattering parameters beyond the Born approximation for arbitrary mass ratio. The correct scattering parameters will be used in Sec. IV C to construct phase diagrams and density profiles for quantitative comparisons with experiments in the BEC regime.

III. BOSON-FERMION AND BOSON-BOSON SCATTERING LENGTHS

Mixtures of two types of fermions in the strong attraction limit can be described by effective Bose-Fermi models [22,26,30,31], where fermion pairs behave as molecular bosons and interact weakly with each other and with excess unpaired fermions. Scattering lengths between two molecular bosons (a_{BB}), and between a molecular boson and an excess fermion (a_{BF}) were calculated in the Born approximation using diagrammatic techniques for equal [13] and unequal masses [26,30]. However, these results do not agree with calculations using few body techniques [35,36], because it is necessary to go beyond the Born approximation.

In the case of fermion mixtures with equal masses, while the Born approximation in many body theory leads to $a_{BB} = 2a_F$ [13] and $a_{BF} = 8a_F/3$ [22,26], the results from few body techniques are $a_{BB} \approx 0.60 a_F$ [35] and $a_{BF} \approx 1.18 a_F$ [37]. However, a diagrammatic approach beyond the Born approximation [38,39] for equal mass fermions recovers the few body results. In this section, we generalize these diagrammatic approaches and analyze the boson-fermion and boson-boson scattering parameters for two types of fermions with unequal masses in order to make quantitative predictions for experiments involving Fermi-Fermi mixtures in the strong attraction limit. Here, we show that the diagrammatic approach for unequal mass fermions produce results consistent with three and four body techniques that were recently used to obtain a_{BF} and a_{BB} as a function of mass ratio [35,36].

We would like to emphasize that our diagrammatic calculation for the scattering parameters of the three and four body

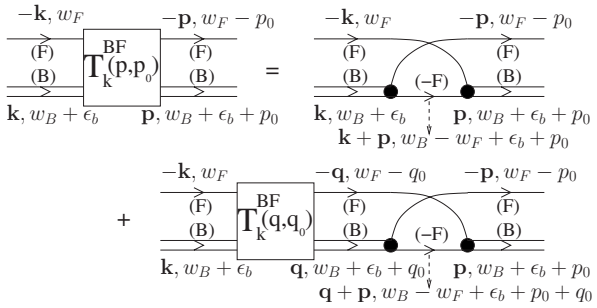

FIG. 1. Diagrammatic representation of the integral equation for the boson-fermion scattering T matrix $T^{BF}_{\mathbf{k}}(\mathbf{p},p_0)$. Here, we use the notation $(-\uparrow)\equiv\downarrow$ and vice versa.

problem is exact. These three and four body diagrammatic results are sufficient to describe ultracold Fermi-Fermi mixtures in the strong attraction limit, since experiments are always performed at low densities. However, the calculation of scattering parameters for three and four fermions in the presence of many others (arbitrary density) is much more difficult, and is not discussed here.

We analyze the technical aspects of the boson-fermion scattering parameter for unequal mass fermions in some detail, since they are much easier to present, while we do not discuss in great detail the technical aspects of the boson-boson scattering parameter for unequal masses, as they are extremely cumbersome. Detailed descriptions of the boson-fermion and boson-boson scattering parameters for equal mass fermions can be found in the literature [38,39].

We begin our analysis by describing a zero temperature ($T=0$) diagrammatic representation for the boson-fermion scattering T matrix $T^{BF}_{\mathbf{k}}(\mathbf{p},p_0)$ as shown in Fig. 1, where $w_F=k^2/(2m_F)$ and $w_B=k^2/(2m_B)$ are the kinetic energies for the excess fermions and molecular bosons, respectively, and $\epsilon_b=-1/(m_{\uparrow\downarrow}a_F^2)<0$ is the binding energy of the molecular bosons. Here,

$$m_B=m_\uparrow+m_\downarrow \tag{2}$$

$$m_{\uparrow\downarrow}=\frac{2m_\uparrow m_\downarrow}{m_\uparrow+m_\downarrow} \tag{3}$$

are masses of the molecular bosons and twice the reduced mass of the $\uparrow$ and $\downarrow$ fermions, respectively. In this figure, single lines represent retarded free fermion propagators

$$G_{0,\sigma}(\mathbf{k},w)=\frac{1}{w-w_\sigma+\mu_\sigma+i0^+}, \tag{4}$$

where $w_\sigma=k^2/(2m_\sigma)$ is the energy and μ_σ is the chemical potential of the σ-type fermions. Similarly double lines represent the retarded molecular boson propagators

$$D_0(\mathbf{k},w)=\frac{4\pi/m_{\uparrow\downarrow}^{3/2}}{|\epsilon_b|^{1/2}-(w_B-w-\mu_\uparrow-\mu_\downarrow-i0^+)^{1/2}} \tag{5}$$

obtained from the expansion of the effective action [26,30], and a corresponding random-phase approximation (RPA) resummation of the fermion polarization bubbles leading to $D_0(\mathbf{k},w)=-g/[1+g\Gamma(\mathbf{k},w)]$ where the fermion polarization bubble is $\Gamma(\mathbf{k},w)=\Sigma_{\mathbf{q},q_0}G_{0,\sigma}(\mathbf{k}+\mathbf{q},w+q_0)G_{0,\sigma}(-\mathbf{q},-q_0)$. Integration over the internal momentum $\mathbf{q}$ and frequency q_0 leads to $\Gamma(\mathbf{k},w)=\Gamma(0,0)+[m_{\uparrow\downarrow}^{3/2}/(4\pi)](w_B-w-\mu_\uparrow-\mu_\downarrow-i0^+)^{1/2}$ which in combination with the definition of the fermion-fermion scattering length $a_F=m_{\uparrow\downarrow}T^{FF}(0,0)/4\pi$, and the fermion-fermion T matrix $T^{FF}(0,0)=-g/[1+g\Gamma(0,0)]$ lead to the final result described in Eq. (5).

On the right hand side of Fig. 1, the first diagram represents a fermion exchange process, and all other (infinitely many) possible processes are included in the second diagram. In all diagrams, we choose $\uparrow(\downarrow)$ to label lighter (heavier) fermions such that lighter (heavier) fermions are in excess when $F\equiv\uparrow(F\equiv\downarrow)$. This choice spans all possible mass ratios. In the following, we set $\mu_\sigma=0$ since all of the calculations are performed for three fermions scattering in vacuum. The T matrix $T^{BF}_{\mathbf{k}}(\mathbf{p},p_0)$ satisfies the following integral equation

$$\begin{aligned}T^{BF}_{\mathbf{k}}(\mathbf{p},p_0)=&-G_{0,-F}(\mathbf{k}+\mathbf{p},w_B-w_F+\epsilon_b+p_0)\\&-\sum_{\mathbf{q},q_0}D_0(\mathbf{q},w_B+\epsilon_b+q_0)G_{0,F}(-\mathbf{q},w_F-q_0)\\&\times T^{BF}_{\mathbf{k}}(\mathbf{q},q_0)G_{0,-F}(\mathbf{p}+\mathbf{q},w_B-w_F+\epsilon_b+p_0+q_0),\end{aligned} \tag{6}$$

where we used $(-\uparrow)\equiv\downarrow$ and vice versa, and $\Sigma_{\mathbf{q},q_0}\equiv i\int d\mathbf{q}\,dq_0/(2\pi)^4$. On the right hand side, we can sum over frequency q_0 by closing the integration contour in the upper half-plane, where $T^{BF}_{\mathbf{k}}(\mathbf{q},q_0)$ and $D_0(\mathbf{q},w_B+\epsilon_b+q_0)$ are analytic functions of q_0. Since this integration sets $q_0=k^2/(2m_F)-q^2/(2m_F)$, we set $p_0=k^2/(2m_F)-p^2/(2m_F)$ in order to have the same frequency dependence for the T matrix on both sides [39]. Since we are interested in the zero-range low energy s-wave scattering, we average out the angular dependences of $\mathbf{k}$ and $\mathbf{p}$. When $k\to0$, the generalized integral equation defined in Eq. (7) can be expressed in terms of the boson-fermion scattering function $a_{k\to0}(p)$ as

$$\begin{aligned}\frac{m_{\uparrow\downarrow}a_0^{BF}(p)/m_{BF}}{a_F^{-1}+(m_{\uparrow\downarrow}p^2/m_{BF}+a_F^{-2})^{1/2}}&=\frac{1}{p^2+a_F^{-2}}-\frac{m_B}{2\pi m_F}\int_0^\infty\frac{dq}{qp}\\&\times\ln\left(\frac{q^2+2m_Fqp/m_B+p^2+a_F^{-2}}{q^2-2m_Fqp/m_B+p^2+a_F^{-2}}\right)a_0^{BF}(q).\end{aligned} \tag{7}$$

Here, we used the definition of the boson-fermion scattering length

$$a_k^{BF}(p)=\frac{m_{BF}}{m_{\uparrow\downarrow}^{3/2}}\left[|\epsilon_b|^{1/2}+\left(\frac{p^2-k^2}{m_{BF}}-\epsilon_b\right)^{1/2}\right]T_k^{BF}(p), \tag{8}$$

with its full momentum dependence, where m_{BF} is twice the reduced mass of an excess fermion and a molecular boson given by

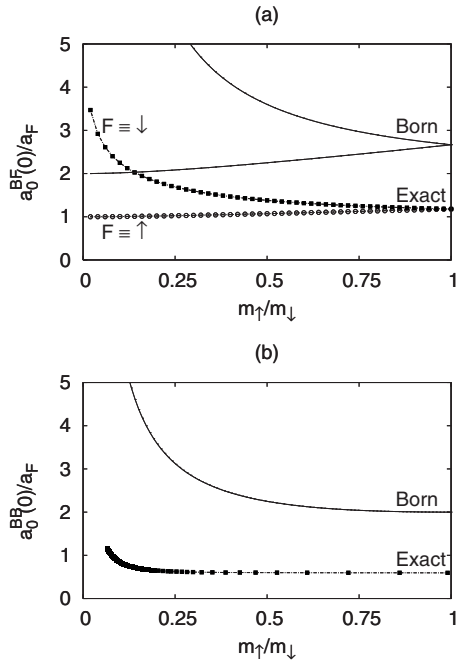

FIG. 2. The boson-fermion scattering length $a_0^{BF}(0)/a_F$ versus mass anisotropy $m_\uparrow/m_\downarrow$ is shown in (a) when lighter ↑-type (hollow circles) or heavier (solid circles) ↓-type fermions are in excess. The boson-boson scattering length $a^{BB}(0)/a_F$ versus mass anisotropy $m_\uparrow/m_\downarrow$ is shown in (b). In addition, the scattering lengths in the Born approximation are shown as solid lines.

$$m_{BF} = \frac{2m_B m_F}{m_B + m_F}. \tag{9}$$

The integral equation shown in Eq. (7) as well as the scattering length expression shown in Eq. (8) reduce to the results for the equal masses [38,39] when $m_\uparrow = m_\downarrow = m$. Notice that only the fermion exchange process is taken into account in the Born approximation, and that neglecting the second term on the right hand side of Eq. (7) leads to $a_0^{BF}(0) = 2(m_{BF}/m_{\uparrow\downarrow})a_F$ which is consistent with our previous results [26,30]. However, we need to include both terms in order to find the exact boson-fermion scattering length.

Next, we solve numerically the integral equation given in Eq. (7), and obtain $a_0^{BF}(p)$ as a function of the mass anisotropy $m_\uparrow/m_\downarrow$. The exact solutions and the Born approximation values of $a_0^{BF}(0)$ are shown in Fig. 2(a). When $m_\uparrow = m_\downarrow$, we find $a_0^{BF}(0) \approx 1.179 a_F$, which is consistent with results previously found for equal masses [31,35–39]. Notice that $a_0^{BF}(0)$ decreases (increases) from this value with increasing mass anisotropy when the lighter (heavier) fermions are in excess. In addition, in the limit of $m_\uparrow/m_\downarrow \to 0$, while $a_0^{BF}(0) \to a_F$ when the lighter fermions are in excess, $a_0^{BF}(0)$ grows rapidly when the heavier fermions are in excess. Notice also that the Born approximation values for $a_0^{BF}(0)$ are not in agreement with the exact values for any mass anisotropy, but the general qualitative trends are captured by the Born approximation as can be seen from Fig. 2(a).

In addition, we present results for $a^{BB}(0)$ as a function of mass anisotropy $m_\uparrow/m_\downarrow$ in Fig. 2(b). The exact results of the boson-boson scattering parameters for unequal mass fermions can be obtained either by extending the diagrammatic approach for equal mass fermions [38,39] or by using few body techniques [35]. The Born approximation values $a^{BB}(0) = (m_B/m_{\uparrow\downarrow})a_F$ are found in Refs. [26,30]. Since the technical details to calculate the boson-boson scattering parameters are quite cumbersome, and not particularly illuminating, here we just mention that the results found in the literature [35] can also be obtained diagrammatically for the unequal mass case. As shown in Fig. 2(b), $a^{BB}(0)$ grows very slowly as the mass ratio $m_\uparrow/m_\downarrow$ decreases, in contrast with the much more rapid growth of the Born approximation values of $a^{BB}(0)$. As expected, the Born approximation values of $a^{BB}(0)$ are not in agreement with the exact values for any mass anisotropy.

TABLE I. Exact boson-boson (a_{BB}) and boson-fermion (a_{BF}) scattering lengths for a list of two-species Fermi-Fermi mixtures. Here, $a_{B\uparrow}$ ($a_{B\downarrow}$) corresponds to excess type of ↑ (↓) fermions.

↑	↓	$m_\uparrow/m_\downarrow$	a_{BB}/a_F	$a_{B\uparrow}/a_F$	$a_{B\downarrow}/a_F$
^{6}Li	^{6}Li	1.000	0.593	1.179	1.179
^{6}Li	^{40}K	0.150	0.695	1.010	1.984
^{6}Li	^{87}Sr	0.068	1.123	1.003	2.512
^{6}Li	^{171}Yb	0.035	—	1.001	3.023
^{40}K	^{40}K	1.000	0.593	1.179	1.179
^{40}K	^{87}Sr	0.460	0.597	1.064	1.411
^{40}K	^{171}Yb	0.234	0.629	1.022	1.723
^{87}Sr	^{87}Sr	1.000	0.593	1.179	1.179
^{87}Sr	^{171}Yb	0.508	0.599	1.073	1.374
^{171}Yb	^{171}Yb	1.000	0.593	1.179	1.179

Several atomic gases of fermions (^{6}Li, ^{40}K, ^{87}Sr [40], and ^{171}Yb [41]) are currently being investigated, and experimental methods for studying mixtures of two types of fermions are being developed in several groups. Thus, anticipating future experiments involving mixtures of two types of fermions, we show in Table I the boson-fermion and boson-boson scattering lengths for a few mixtures.

Here, we make two comments. First, it is quite remarkable that the diagrammatic approach recovers the few body results for boson-fermion and boson-boson scattering lengths for arbitrary mass ratio $m_\uparrow/m_\downarrow$. The diagrammatic approach is performed in momentum space, while the few body approach is performed in real space. The two methods are equivalent because all of the possible scattering processes are taken into account exactly in the diagrammatic approach at $T=0$ for three or four fermions. However, the calculation of the scattering parameters for three or four fermions in the presence of many others (arbitrary number of particles) at zero or finite temperatures requires a full many body approach, which is inevitably approximate and more difficult to implement. Second, our analysis does not include the effects related to Efimov (three body bound) states, which may become important when analyzing the scattering parameters as a function of mass ratio $m_\uparrow/m_\downarrow$ [36]. In particular, the mixtures of ^{6}Li and ^{87}Sr or ^{6}Li and ^{171}Yb have mass ratios of $m_{\mathrm{Li}}/m_{\mathrm{Sr}} \approx 0.068$ and $m_{\mathrm{Li}}/m_{\mathrm{Yb}} \approx 0.035$, which are below the

critical ratio $m_\uparrow/m_\downarrow \approx 0.073$ for the emergence of Efimov states.

Having presented the boson-fermion and boson-boson scattering lengths for arbitrary mass ratio $m_\uparrow/m_\downarrow$, we discuss next the resulting phase diagrams for Fermi-Fermi mixtures in the strong attraction limit, where the system can be effectively described by a Bose-Fermi mixture [22,26,30,31] of molecular bosons and excess unpaired fermions.

IV. BOSE-FERMI MIXTURES AT ZERO TEMPERATURE

In this section we use the effective Bose-Fermi mixture description [22,26,31] to analyze the phase diagram of population imbalanced Fermi-Fermi mixtures in the strong attraction limit. We describe first the general stability conditions for Bose-Fermi mixtures at zero temperature, and use this connection to discuss the stability and phase diagrams of Fermi-Fermi mixtures in the strong attraction limit.

A. Weakly interacting atomic Bose-Fermi mixtures

The ground state of Bose-Fermi mixtures can be described by the free energy density [30,42]

$$\varepsilon = \varepsilon_B + \varepsilon_F + \frac{U_{BB} n_B^2}{2} + U_{BF} n_F n_B - \mu_F n_F - \mu_B n_B, \quad (10)$$

which characterizes the center-of-mass degrees of freedom for a mixture of single-hyperfine-state bosons and fermions. Here μ_F and n_F (μ_B and n_B) are the density and chemical potential of fermions (bosons), ϵ_F is the Fermi energy of the fermions, and U_{BB} and U_{BF} are the repulsive boson-boson and boson-fermion interaction strengths, which have dimensions of energy times volume in 3D. The density of single-hyperfine-state fermions in three dimensions is given by $n_F = (1/V)\Sigma_{\mathbf{k}}^{|\mathbf{k}|<k_F} 1 = k_F^3/(6\pi^2)$, where k_F is the Fermi momentum and V is the volume. The first term in Eq. (10) is the total kinetic energy of bosons, which is assumed to be much smaller than all other energies, and is neglected. This assumption is very good since essentially all bosons are condensed in the $\mathbf{k}=\mathbf{0}$ state, when the boson-boson and boson-fermion interactions are weak. The second term in Eq. (10) is the total kinetic energy of fermions, which in three dimensions is given by $\varepsilon_F = (1/V)\Sigma_{\mathbf{k}}^{|\mathbf{k}|<k_F} \epsilon_{\mathbf{k},F} = 3\epsilon_F n_F/5$, where $\epsilon_{\mathbf{k},F} = |\mathbf{k}|^2/(2m_F)$.

From the free energy given in Eq. (10), we obtain the fermion and boson chemical potentials using the condition $\partial\varepsilon/\partial n_i = 0$ with $i \equiv \{F, B\}$, leading to

$$\mu_F = \epsilon_F + U_{BF} n_B, \quad (11)$$

$$\mu_B = U_{BB} n_B + U_{BF} n_F. \quad (12)$$

Then, we use the positive definiteness of the Bose-Fermi compressibility matrix $\kappa_{i,j} = \partial\mu_i/\partial n_j$,

$$\frac{\partial\mu_F}{\partial n_F}\frac{\partial\mu_B}{\partial n_B} - \frac{\partial\mu_F}{\partial n_B}\frac{\partial\mu_B}{\partial n_F} > 0, \quad (13)$$

and find that bosons and fermions phase separate when the condition

$$n_F \geqslant \frac{4\pi^4}{3m_F^3}\frac{U_{BB}^3}{U_{BF}^6}, \quad \text{(3D)} \quad (14)$$

is satisfied in three-dimensional systems [30,42]. Therefore, the stability of uniform superfluidity puts an upper limit on the density of fermions in three-dimensions.

Following a similar approach in lower dimensions, where $n_F = k_F^2/(4\pi)$ and $\varepsilon_F = \epsilon_F n_F/2$ in two dimensions, and $n_F = k_F/\pi$ and $\varepsilon_F = \epsilon_F n_F/3$ in one dimension, we find that the bosons and the fermions phase separate when the conditions

$$1 \leqslant \frac{m_F}{2\pi}\frac{U_{BF}^2}{U_{BB}}, \quad \text{(2D)} \quad (15)$$

$$n_F \leqslant \frac{m_F}{\pi^2}\frac{U_{BF}^2}{U_{BB}}, \quad \text{(1D)} \quad (16)$$

are satisfied, respectively, for two- and one-dimensional systems. Notice that the stability of uniform superfluidity puts a lower limit in one dimension, which is in sharp contrast with the three-dimensional result. Furthermore, the stability condition in two dimensions does not depend explicitly on the density of fermions (see also Ref. [43]). However, the results in lower dimensions have to be used with caution, since quantum fluctuations are more pronounced, and may affect these stability conditions.

For an atomic Bose-Fermi mixture, we can also describe analytically a finer structure of phases. There are four possible phases [42]: (i) PS(1) where there is phase separation between pure fermions and pure bosons; (ii) PS(2) where there is phase separation between pure fermions, and a mixture of fermions and bosons; (iii) PS(3) where there is phase separation between pure bosons, and a mixture of fermions and bosons; and (iv) PS(4) where there is phase separation between two different mixtures of fermions and bosons.

For a three-dimensional weakly interacting Bose-Fermi mixture, we follow Ref. [42] and find that there are only two stable phases within the phase separation region: (i) PS(1) where there is phase separation between pure fermions and pure bosons, and (ii) PS(2) where there is phase separation between pure fermions, and a mixture of fermions and bosons. We obtain analytically the condition

$$n_F \geqslant \frac{1125\pi^4}{128m_F^3}\frac{U_{BB}^3}{U_{BF}^6} - \frac{5}{4}\frac{U_{BB}}{U_{BF}} n_B, \quad \text{(3D)} \quad (17)$$

for the transition from the PS(2) to the PS(1) phase [30].

In lower dimensions, we find that the structure of the phase diagram is quite different. In two dimensions, the phase separated region consists only of PS(1) where there is phase separation between pure fermions and pure bosons. While, for a one-dimensional weakly interacting Bose-Fermi mixture, the phase-separated region consists also of two regions: (i) PS(1) where there is phase separation between pure fermions and pure bosons, and (iii) PS(3) where there is phase separation between pure bosons, and a mixture of fermions and bosons. We obtain analytically the condition

$$n_F \leqslant \frac{3m_F}{2\pi^2}\frac{U_{BF}^2}{U_{BB}} - \frac{U_{BB}}{U_{BF}}n_B, \quad \text{(1D)} \tag{18}$$

for the transition from the PS(3) to the PS(1) phase. Notice that the structure of the PS(3) phase in one dimension is very different from the structure of the PS(2) phase in three dimensions. Again, the results in lower dimensions have to be used with caution, since the quantum fluctuations are more pronounced, and may affect these stability conditions.

Next, we concentrate only on the three-dimensional case, and use the stability conditions found above as well as the interaction (scattering) parameters obtained in Sec. III to analyze the phase diagrams of Fermi-Fermi mixtures in the strong attraction limit.

B. Fermi-Fermi mixtures in the strong attraction limit

To make an analogy between Bose-Fermi mixtures and population imbalanced Fermi-Fermi mixtures in the strong attraction limit, we identify $F \equiv \{\uparrow \text{ or } \downarrow\}$ as the excess fermions. This identification leads to the density of excess fermions (n_E) and molecular bosons (n_B) given by

$$n_E = n_F - n_{-F} = |n_\uparrow - n_\downarrow|, \tag{19}$$

$$n_B = \frac{n - n_E}{2} = n_{-F}, \tag{20}$$

respectively, where $n=n_\uparrow+n_\downarrow$ is the total density of $\uparrow$- and $\downarrow$-type fermions. Here, we use $(-\uparrow) \equiv \downarrow$ and vice versa. For instance, if $F \equiv \uparrow$ fermions are in excess, the density of excess fermions and molecular bosons are $n_E=n_\uparrow-n_\downarrow$ and $n_B=(n-n_E)/2=n_\downarrow$, respectively, such that all $\downarrow$-type fermions are paired with some of the $\uparrow$-type fermions to form molecular bosons, but there are $\uparrow$-type fermions left unpaired. It is important to emphasize that the internal degrees of freedom (electronic, vibrational, and rotational) of molecular bosons are not explicitly considered here, in the same spirit of the description of atomic bosons presented in Sec. IV A, where the electronic degrees of freedom were also not explicitly considered.

For three dimensions, we define the boson-boson and boson-fermion interaction strengths

$$U_{BB} = \frac{4\pi a_{BB}}{m_B} = \frac{4\pi\gamma_B}{m_B}a_F, \tag{21}$$

$$U_{BF} = \frac{4\pi a_{BF}}{m_{BF}} = \frac{4\pi\beta_F}{m_{BF}}a_F, \tag{22}$$

where a_F, $a_{BB}=\gamma_B a_F$, and $a_{BF}=\beta_F a_F$ are the fermion-fermion, boson-boson, and boson-fermion scattering lengths. Here, $\gamma_B=a_{BB}/a_F$ and $\beta_F=a_{BF}/a_F$ are constants, which are found in Sec. III as shown in Fig. 2 and Table I. In addition, we define the population imbalance parameter

$$P = \frac{N_\uparrow - N_\downarrow}{N_\uparrow + N_\downarrow} = \frac{n_\uparrow - n_\downarrow}{n_\uparrow + n_\downarrow}, \tag{23}$$

such that $|P|=n_E/n$, and $n=K_F^3/(3\pi^2)$, where N_σ is the number of σ-type fermions and K_F is the Fermi momentum corresponding to the total density of fermions defined by $K_F^3=(k_{F,\downarrow}^3+k_{F,\uparrow}^3)/2$.

Using these definitions, the phase separation condition Eq. (14) becomes

$$|P| \geqslant \frac{\pi^3\gamma_B^3 m_{BF}^6}{16\beta_F^6 m_B^3 m_F^3}\lambda^3, \tag{24}$$

where $\lambda=1/(K_F a_F)$ is the scattering parameter. Similarly, the condition given in Eq. (17) becomes

$$|P|\left(1 - \frac{5\gamma_B m_{BF}}{8\beta_F m_B}\right) \geqslant \frac{3375\pi^3\gamma_B^3 m_{BF}^6}{8192\beta_F^6 m_B^3 m_F^3}\lambda^3 - \frac{5\gamma_B m_{BF}}{8\beta_F m_B}, \tag{25}$$

for the transition from the PS(2) to the PS(1) phase.

We emphasize that these analytic expressions given in Eqs. (24) and (25) are valid only in the strong attraction limit when $1/(K_F a_F) \gg 1$, but they may still give semiquantitative results for $1/(K_F a_F) \gtrsim 1$. Close to the unitarity, the Bose-Fermi description of Fermi-Fermi mixtures in terms of molecular bosons and excess fermions is not reliable, since the binding energy of molecular bosons is small and the interactions between molecular bosons and excess fermions or between two molecular bosons may be sufficient to cause dissociation of the molecules into directly scattering fermions. However, there may be an intermediate regime between unitarity and the strict BEC limit where we can describe Fermi-Fermi mixtures in terms of a mixture of molecular bosons and excess fermions such that the molecular bosons can dissociate due to boson-boson or boson-fermion interactions, but be in chemical equilibrium with excess fermions. When dissociation of molecular bosons is included, the system is no longer a binary mixture of molecular bosons and excess fermions, but a ternary mixture of molecular bosons, dissociated bosons ($\uparrow\downarrow \rightleftharpoons \uparrow + \downarrow$), and excess fermions, or effectively a ternary mixture of molecular bosons, and $\uparrow$- and $\downarrow$-type fermions. In the case of ternary mixtures, there can be a large number of phase separated regimes. If we confine our discussion to the equilibrium of a maximum of two phases of this ternary mixture then several other situations can be encountered. For example, when $\downarrow$-type fermions are in excess, a possible sequence of phases for fixed population imbalance P and increasing scattering parameter $1/(K_F a_F)$ is (1) Normal phase (N) of partially polarized fermions $\rightarrow$ (2) mixture of molecular bosons and $\uparrow$-type fermions phase separated from partially polarized normal fermions $\rightarrow$ (3) molecular bosons phase separated from excess $\downarrow$-type fermions $\rightarrow$ (4) mixture of molecular bosons and $\downarrow$-type excess fermions phase separated from $\downarrow$-type excess fermions $\rightarrow$ (5) coexistence of molecular bosons and $\downarrow$-type excess fermions.

Therefore, as long as Fermi-Fermi mixtures can be regarded as a binary mixture of nondissociated molecular bosons and excess fermions, the expressions given in Eqs. (24) and (25) may be used as a guide for the boundaries between phase separated (nonuniform) and the mixed (uniform) phases for any mixture of fermions. In particular, Eqs. (24) and (25) may serve as estimators for the phase boundaries of equal or unequal mass Fermi-Fermi mixtures with population imbalance, as discussed next.

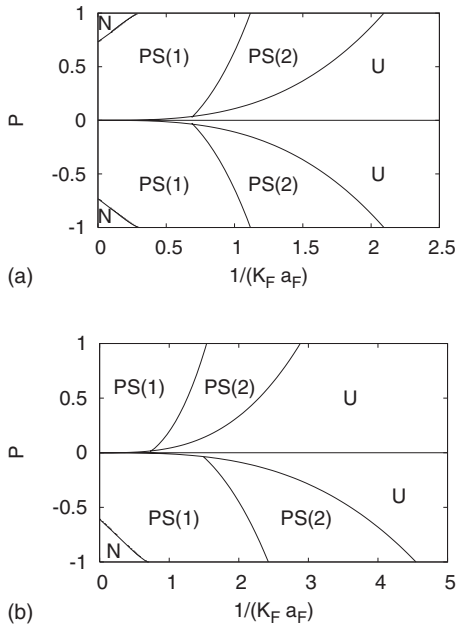

FIG. 3. Phase diagram of population imbalance $P=(n_\uparrow-n_\downarrow)/(n_\uparrow+n_\downarrow)$ versus scattering parameter $1/(K_Fa_F)$ for (a) equal masses when $m_\uparrow=m_\downarrow$, and (b) unequal masses when $m_\uparrow=0.15m_\downarrow$ in the BEC side. We show normal (N), uniform superfluid (U), and phase-separated nonuniform superfluid phases PS(1) and PS(2).

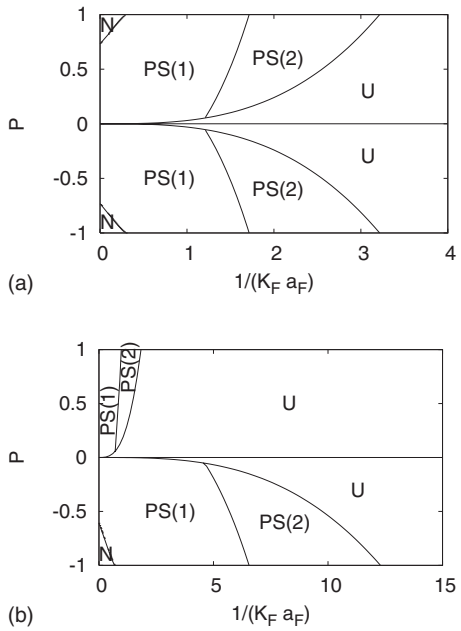

FIG. 4. Phase diagram of population imbalance $P=(n_\uparrow-n_\downarrow)/(n_\uparrow+n_\downarrow)$ versus scattering parameter $1/(K_Fa_F)$ in the Born approximation for (a) equal masses when $m_\uparrow=m_\downarrow$, and (b) unequal masses when $m_\uparrow=0.15m_\downarrow$ in the BEC side. We show normal (N), uniform superfluid (U), and phase-separated nonuniform superfluid phases PS(1) and PS(2).

C. Phase diagrams of Fermi-Fermi mixtures in the strong attraction limit

Among many possibilities of Fermi-Fermi mixtures (see Table I), we focus our analysis on population imbalanced mixtures of ^{6}Li or ^{40}K atoms where $m_\uparrow=m_\downarrow$, and ^{6}Li and ^{40}K atoms where $m_\uparrow=0.15m_\downarrow$.

In Fig. 3, we show phase diagrams of population imbalance P and scattering parameter $1/(K_Fa_F)$ for equal mass mixtures when $m_\uparrow=m_\downarrow$, and for unequal mass mixtures when $m_\uparrow=0.15m_\downarrow$. In these diagrams, we choose $\uparrow$ ($\downarrow$) to label lighter (heavier) fermions such that lighter (heavier) fermions are in excess when $P>0$ ($P<0$). Although these diagrams are strictly valid in the strong attraction limit when $1/(K_Fa_F)\gg 1$, they are qualitatively correct when $1/(K_Fa_F)\gtrsim 1$ or as long as the molecular bosons are not dissociated. In the later case, the system may be approximately described as a ternary mixture of molecular bosons, $\uparrow$- and $\downarrow$-type fermions and many other phases are possible, as discussed in Sec. IV B.

In these figures, we show the following phases: (i) the normal (N) phase corresponding to balanced ($P=0$) or imbalanced ($P\neq 0$) mixture of unpaired $\uparrow$- or $\downarrow$-type fermions; (ii) uniform superfluid (U) phase where paired (molecular bosons) and unpaired fermions coexist; and (iii) PS nonuniform superfluid phases. The PS(1) region labels phase separation between pure excess fermions and superfluid molecular bosons, while the PS(2) region labels phase separation between pure excess fermions, and a mixture of excess fermions and superfluid molecular bosons. The phase boundary between U and PS(2) phases is determined from Eq. (24), and the phase boundary between PS(2) and PS(1) phases is determined from Eq. (25). For a fixed mass anisotropy, when $|P|$ is large, we find phase transitions from PS(1)$\rightarrow$PS(2)$\rightarrow U$ as the interaction strength $1/(K_Fa_F)$ increases. However, when $|P|$ is very small, we find a phase transition directly from the PS(1) to the U phase as $1/(K_Fa_F)$ increases.

We remark in passing that the phase diagrams for mixtures of ^{6}Li and ^{87}Sr or ^{6}Li and ^{171}Yb with mass ratios of $m_{\mathrm{Li}}/m_{\mathrm{Sr}}\approx 0.068$ and $m_{\mathrm{Li}}/m_{\mathrm{Yb}}\approx 0.035$, which are below the critical ratio $m_\uparrow/m_\downarrow\approx 0.073$ for the emergence of Efimov (three body bound) states are much richer, since phase separation and coexistence phases involving Efimov states (trimers), molecular bosons and excess fermions are also present.

It is also important to emphasize that since we use the exact boson-boson and boson-fermion scattering lengths, our phase diagrams in the strong attraction limit already include fluctuation corrections beyond the Born approximation. For comparison, the corresponding phase diagrams within the Born approximation are described in Fig. 4, where the phase boundaries in the population imbalance P versus scattering parameter $1/(K_Fa_F)$ plane are shown for equal ($m_\uparrow=m_\downarrow$) and unequal ($m_\uparrow=0.15m_\downarrow$) mass mixtures. A direct comparison of Figs. 3 and 4 shows that the results beyond the Born approximation are quantitatively different from the saddle-point results [19,20] in the equal mass case. These quantitative differences become significantly large for unequal mass mixtures when heavier fermions are in excess [26,30,32,34] due to the large sensitivity of the exact scattering parameters on the mass ratio $m_\uparrow/m_\downarrow$ as shown in Fig. 2 and Table I. However, the same phases are present in both cases, indicating that the Born approximation captures the basic qualitative features, but fails to produce the phase boundaries quantitatively.

Lastly, we point out the presence of several triple points in the phase diagrams shown in Figs. 3 and 4. Along the $|P|=1$ lines, we find several triple points as $1/(K_F a_F)$ increases where the fully polarized normal phases ($P=\pm 1$) merge with (i) the partially polarized normal (N) and the PS(1) phase; or with (ii) the PS(1) and PS(2) phases; or with (iii) the PS(2) and U phases. Furthermore, there is also an additional triple point that occurs for small $|P|$ (iv) where the phases PS(1), PS(2), and U meet. The precise locations of these triple points can be obtained for any mass ratio and scattering parameter from Eqs. (24) and (25) using the equal sign (=) condition. The triple point for case (ii) can be obtained by setting $|P|=1$ in Eq. (25), and the triple point for case (iii) can be obtained by setting $|P|=1$ in Eq. (24). Finally, the triple point for case (iv) can be obtained by using the equal sign (=) condition of Eqs. (24) and (25) and by solving the two equations simultaneously.

Having analyzed the phase diagrams for nontrapped continuous systems, we discuss next the effects of the trapping potential which are necessary to understand experiments involving ultracold Fermi-Fermi mixtures.

V. TRAPPED BOSE-FERMI MIXTURES AT ZERO AND FINITE TEMPERATURES

In this section, we use again the simpler description of the effective Bose-Fermi mixture to describe trapped Fermi-Fermi mixtures in the strong attraction limit. For this purpose, we present first the theory of trapped Bose-Fermi mixtures at zero and finite temperatures, and then discuss the density profiles of trapped Fermi-Fermi mixtures in the strong attraction limit using the relation between the two systems described in Sec. IV.

A. Weakly interacting atomic Bose-Fermi mixtures

The Hamiltonian density for a Bose-Fermi mixture in an external potential can be written as

$$H(\mathbf{r}) = K_F(\mathbf{r}) + V_F(\mathbf{r})\hat{n}_F(\mathbf{r}) + K_B(\mathbf{r}) + V_B(\mathbf{r})\hat{n}_B(\mathbf{r}) + U_{BF}\hat{n}_B(\mathbf{r})\hat{n}_F(\mathbf{r}) + (U_{BB}/2)\hat{n}_B(\mathbf{r})\hat{n}_B(\mathbf{r}), \quad (26)$$

where $K_i(\mathbf{r}) = \psi_i^\dagger(\mathbf{r})[-\nabla^2/(2m_i) - \mu_i]\psi_i(\mathbf{r})$ represents the kinetic and chemical potential terms for fermions ($i \equiv F$) or bosons ($i \equiv B$) in a single hyperfine state. Here, $\hat{n}_i(\mathbf{r}) = \psi_i^\dagger(\mathbf{r})\psi_i(\mathbf{r})$ represent the local density operators, and U_{BF} and U_{BB} represent the boson-fermion and boson-boson interaction. The single-hyperfine-state fermions are noninteracting, but obey the Pauli exclusion principle.

For simplicity, we approximate the trapping potential by an isotropic harmonic function where the potential energy is

$$V_i(\mathbf{r}) = \frac{1}{2}\alpha_i r^2. \quad (27)$$

Here, $\alpha_i = m_i\omega_i^2$ is proportional to the trapping frequency of bosons ($i \equiv B$) or fermions ($i \equiv F$), which is typically different for each kind of atom. Since the potential and the interactions are isotropic, the effective potentials and densities depend only on $r = |\mathbf{r}|$.

In the presence of such trapping potentials, the bosons and fermions feel the effective potentials

$$V_{B,\mathrm{eff}}(r) = V_B(r) + 2U_{BB}n_B(r) + U_{BF}n_F(r), \quad (28)$$

$$V_{F,\mathrm{eff}}(r) = V_F(r) + U_{BF}n_B(r), \quad (29)$$

respectively, where $n_F(r)$ is the local density of fermions, and

$$n_B(r) = n_C(r) + n_{NC}(r) \quad (30)$$

is the total local density of bosons. Here, $n_C(r)$ and $n_{NC}(r)$ are the density of condensed and noncondensed bosons, respectively.

The number of condensed bosons is determined from the Gross-Pitaevskii equation leading to

$$n_C(r) = \frac{\mu_B - V_B(r) - 2U_{BB}n_{NC}(r) - U_{BF}n_F(r)}{U_{BB}} \quad (31)$$

within the Thomas-Fermi approximation (TFA), where the kinetic energy of the bosons is neglected. This relation is valid when the condition $\mu_B - V_B(r) - 2U_{BB}n_{NC}(r) - U_{BF}n_F(r) \geq 0$ is satisfied, otherwise, $n_C(r) = 0$.

For a weakly interacting mixture of bosons and fermions, we may use the Hartree-Fock approximation [44] and treat both the noncondensed bosons and fermions as moving in their effective potentials given by Eqs. (28) and (29), respectively. Notice that the exact boson-boson and boson-fermion interactions appear through the effective (renormalized) chemical potentials in this approximation, which works well for the weakly interacting and low density systems considered here. In addition, we assume that noncondensed bosons are in thermal equilibrium with condensed bosons at the same chemical potential μ_B. Within these approximations, the density of noncondensed bosons and fermions are given by

$$n_{NC}(r) = \frac{1}{V}\sum_{\mathbf{k}} b[\epsilon_{\mathbf{k},B} - \mu_B + V_{B,\mathrm{eff}}(r)], \quad (32)$$

$$n_F(r) = \frac{1}{V}\sum_{\mathbf{k}} f[\epsilon_{\mathbf{k},F} - \mu_F + V_{F,\mathrm{eff}}(r)], \quad (33)$$

where $b(x) = 1/[\exp(x/T) - 1]$ is the Bose, and $f(x) = 1/[\exp(x/T) + 1]$ is the Fermi distribution. Here, $\epsilon_{\mathbf{k},i} = |\mathbf{k}|^2/(2m_i)$ is the kinetic energy of bosons ($i \equiv B$) or fermions ($i \equiv F$).

Notice that, at zero temperature, all bosons condense such that $n_{NC}(r) = 0$, and $n_B(r) = n_C(r)$, leading to

$$n_B(r) = \frac{\mu_B - V_B(r) - U_{BF}n_F(r)}{U_{BB}}, \quad (34)$$

$$n_F(r) = \frac{\{2m_F[\mu_F - V_F(r) - U_{BF}n_B(r)]\}^{3/2}}{6\pi^2}, \quad (35)$$

for the densities of bosons and fermions, respectively [30]. The first expression is valid when the condition $\mu_B - V_B(r) - U_{BF}n_F(r) \geq 0$ is satisfied, otherwise, $n_B(r) = 0$. The second expression is valid when the condition $\mu_F - V_F(r)$

$-U_{BF}n_B(r) \geq 0$ is satisfied, otherwise, $n_F(r)=0$.

The chemical potentials of bosons and fermions are determined from fixing the number of bosons and fermions, independently, as follows:

$$N_B = \int d^3r n_B(r), \tag{36}$$

$$N_F = \int d^3r n_F(r), \tag{37}$$

where the integration is over all space. Therefore, in order to find the density profiles for condensed and noncondensed bosons, as wells as for fermions, we need to solve Eqs. (36) and (37) for μ_B and μ_F self-consistently. Next, we discuss the density profiles of Fermi-Fermi mixtures in the strong attraction limit using the effective Bose-Fermi description presented.

B. Fermi-Fermi mixtures in the strong attraction limit

To make the connection between Bose-Fermi mixtures and population imbalanced Fermi-Fermi mixtures in the strong attraction limit, we identify $F \equiv \{\uparrow \text{ or } \downarrow\}$ as the excess fermions. This identification leads to the density of excess fermions (n_E) and molecular bosons (n_B) given by

$$n_E(r) = n_F(r) - n_{-F}(r) = |n_\uparrow(r) - n_\downarrow(r)|, \tag{38}$$

$$n_B(r) = \frac{n(r) - n_E(r)}{2} = n_{-F}(r), \tag{39}$$

respectively, where $n(r)=n_\uparrow(r)+n_\downarrow(r)$ is the total density of $\uparrow$- and $\downarrow$-type fermions. Here, we use $(-\uparrow) \equiv \downarrow$ and vice versa. For instance, if $F \equiv \uparrow$ fermions are in excess, the density of excess fermions and molecular bosons are $n_E(r) = n_\uparrow(r) - n_\downarrow(r)$ and $n_B(r) = [n(r) - n_E(r)]/2 = n_\downarrow(r)$, respectively, such that all $\downarrow$-type fermions are paired with some of the $\uparrow$-type fermions to form molecular bosons, but there are $\uparrow$-type fermions left unpaired. In addition, we identify $\alpha_B = \alpha_\uparrow + \alpha_\downarrow$, where $\alpha_\sigma = m_\sigma \omega_\sigma^2$ is different for different atoms.

As an example, we look at the equal mass case $m_F = m_\uparrow = m_\downarrow = m$ and $m_B = m_\uparrow + m_\downarrow = 2m$, and solve the self-consistent relations Eqs. (36) and (37) for a two-hyperfine-state mixture of ^{6}Li only or ^{40}K only. In our numerical analysis, we choose $\alpha_F = \alpha_\uparrow = \alpha_\downarrow = \alpha$ and $\alpha_B = 2\alpha$, scattering parameter $1/(K_F a_F) = 2$ and population imbalance parameter $P=0.5$ such that $n_\uparrow = 3n_\downarrow$. We define a characteristic energy $E_F = K_F^2/(2m)$ in terms of the wave vector K_F and the fermion mass m and assume it to be the known Fermi energy of a gas of noninteracting fermions in the trapping potential $V_F(r)$. We scale the radial distance with the effective Thomas-Fermi (TF) radius R_{TF} defined by $E_F = \alpha R_{TF}^2/2$. With this identification, the total number of trapped fermions $N = (E_F/\omega_F)^3/3$, with $\omega_F = \sqrt{\alpha/m}$, can be rewritten as $N = K_F^3 R_{TF}^3/24$ in terms of K_F and R_{TF}.

Since we are interested also in the temperature dependence of the density profiles, we recall that the critical temperature for Bose-Einstein condensation of a noninteracting harmonically trapped Bose gas is $T_{BEC} = \omega_B [N_B/\zeta(3)]^{1/3}$, where $\omega_B = \sqrt{\alpha_B/m_B}$. In our Fermi-Fermi mixture the number of bosons is $N_B = N(1-|P|)/2$ expressed in terms of the total number of fermions $N = N_\uparrow + N_\downarrow$ and population imbalance $P = (N_\uparrow - N_\downarrow)/N$. Using the expression for N_B, the expression of N in terms of E_F and ω_F, and that $\omega_B = \omega_F$ for equal masses, we find

$$T_{BEC} = \left[\frac{1-|P|}{6\zeta(3)}\right]^{1/3} E_F \approx 0.518(1-|P|)^{1/3} E_F, \tag{40}$$

for the critical BEC temperature, which is valid when $1/(K_F a_F) \to \infty$. Here, $\zeta(x)$ is the zeta function and $\zeta(3) \approx 1.202$. Therefore, for $P=0.5$, we obtain $T_{BEC} \approx 0.41 E_F$. Notice that T_{BEC} for population imbalance P given in Eq. (40) is a generalization of the results for equal populations [45,46].

In Fig. 5, we show the density (in units of K_F^3) of condensed (n_C) and noncondensed (n_{NC}) molecular bosons, and excess (n_E) fermions as a function trap radius r/R_{TF} for four temperatures: (a) $T=0$, (b) $T=0.2E_F$, (c) $T=0.35E_F$, and (d) $T=0.41E_F$. At zero temperature ($T=0$), as shown in Fig. 5(a), we find that all of the molecular bosons are condensed, and that they are concentrated close to the center of the trap. In contrast, the majority of excess fermions are pushed away from the center towards the edges of the trap due to the repulsive boson-fermion interaction and the high concentration of condensed molecular bosons. Therefore, there is a clear indication of phase separation between molecular bosons and excess fermions. When the temperature is increased to $T=0.2E_F$ shown in Fig. 5(b), some of the molecular bosons are not condensed. These noncondensed molecular bosons are also pushed away from the center towards the edges of the trap just like the excess fermions. Further increase in temperature increases (decreases) the number of noncondensed (condensed) molecular bosons as can be seen in Fig. 5(c). For temperatures close to T_{BEC} and above, all of the molecular bosons become noncondensed, as shown in Fig. 5(d), having a Gaussian-like density distribution. Similarly, the excess fermions also have Gaussian-like density distribution for temperatures at T_{BEC} and above due to the absence of the condensate.

Therefore, at zero temperature, we find that the trapping potential tends to favor phase separation into a PS(1)-rich phase where regions of almost pure fermions and almost pure bosons are separated. However, at finite temperatures, the system develops a PS(2)-rich phase where regions of almost pure fermions and of almost fully mixed bosons and fermions are separated. The region of coexistence of bosons and fermions can be further broken down into a domain of coexisting excess fermions with condensed and noncondensed bosons, and into a domain of coexisting excess fermions and noncondensed bosons as can be seen in Fig. 5(d). Again, if the molecular bosons are allowed to dissociate, the system can be described by a ternary mixture as discussed in Sec. IV B and the phase diagram can be even richer, especially closer to the unitarity.

In Fig. 6, we show the density (in units of K_F^3) of $\uparrow$- ($n_\uparrow$) and $\downarrow$-type ($n_\downarrow$) fermions as a function of radius r/R_{TF} for

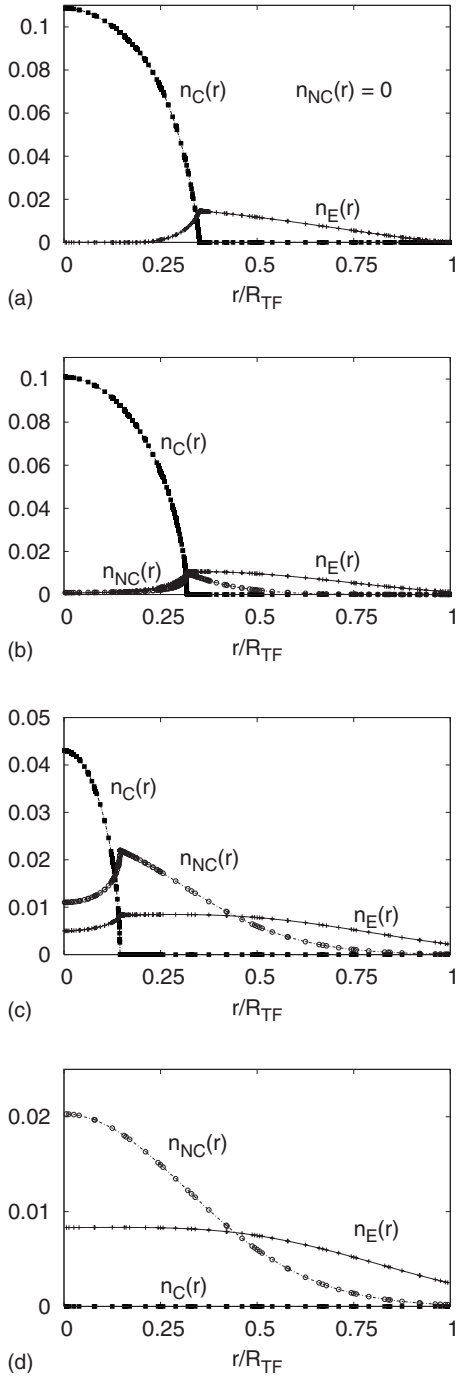

FIG. 5. Density (in units of K_F^3) of condensed (n_C) and noncondensed (n_{NC}) molecular bosons, and excess (n_E) fermions versus trap radius r/R_{TF} is shown for (a) $T=0$, (b) $T=0.2E_F$, (c) $T=0.35E_F$, and (d) $T=0.41E_F$. Here, $m_\uparrow=m_\downarrow$, the population imbalance parameter is $P=0.5$ and the scattering length parameter is $1/(K_F a_F)=2$.

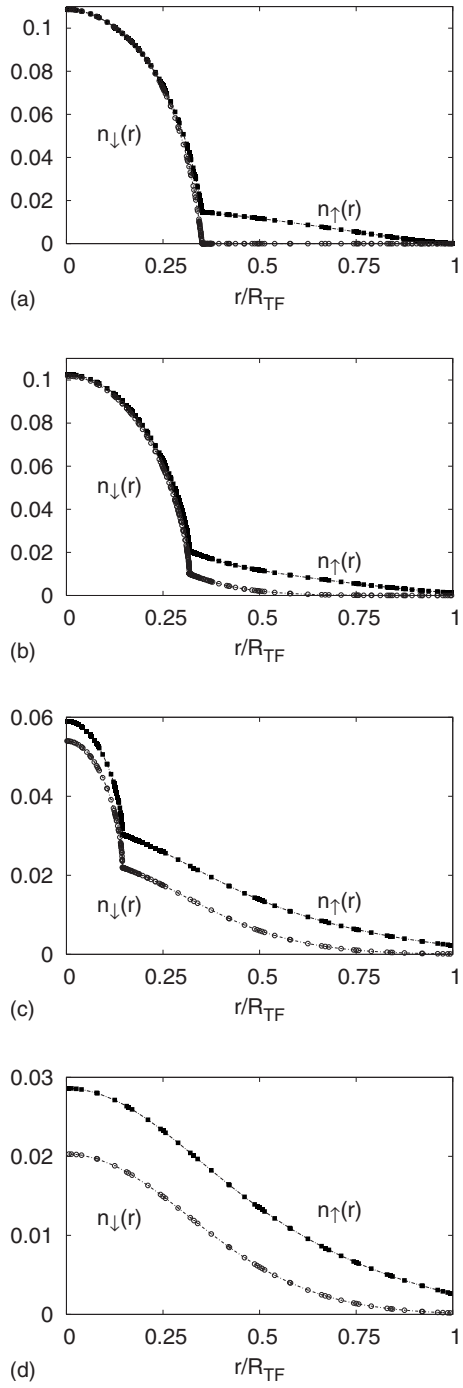

FIG. 6. Density (in units of K_F^3) of ↑- ($n_\uparrow$) and ↓-type ($n_\downarrow$) fermions versus trap radius r/R_{TF} is shown for (a) $T=0$, (b) $T=0.2E_F$, (c) $T=0.35E_F$, and (d) $T=0.41E_F$. Here, $m_\uparrow=m_\downarrow$, population imbalance parameter is $P=0.5$ and scattering length parameter is $1/(K_F a_F)=2$.

four temperatures: (a) $T=0$, (b) $T=0.2E_F$, (c) $T=0.35E_F$, and (d) $T=0.41E_F$. At zero temperature, as shown in Fig. 6(a), we find that the density of ↑- and ↓-type fermions are similar close to the center of the trapping potential, while some of the excess-type fermions are close to the edges. When the temperature increases to $T=0.2E_F$ shown in Fig. 6(b) or to $T=0.35E_F$ shown in Fig. 6(c), the density of ↑- and ↓-type fermions become different at the center of the trap. In addition, both ↑- and ↓-type fermions exist towards the edges. At temperatures close to T_{BEC} and above, the density profiles of ↑- and ↓-type fermions have the standard shapes of weakly interacting trapped Fermi gases.

In this section, we have shown that the effective Bose-Fermi description of Fermi-Fermi mixtures is applicable in

the strong attraction limit, and thus can provide good quantitative comparisons to experiments in the same regime, since the exact boson-fermion and boson-boson scattering parameters were used to obtain the phase diagrams and density profiles. Thus, we think that it is particularly important to perform experiments for different population imbalances in the strong attraction limit, where the theory is simple. The situation is somewhat more complicated near unitarity where quantitative comparisons between theory and experiment are more difficult. Furthermore, there are also some differences between the experimental studies that the Massachusetts Institute of Technology (MIT) [7,9] and Rice University [8,10] groups performed near unitarity, since the shapes of their traps and the number of trapped atoms are quite different.

Having concluded the analysis of the effects of trapping potentials on Fermi-Fermi mixtures in the strong attraction limit, next we give a summary of our conclusions.

VI. CONCLUSIONS

In summary, we used the effective Bose-Fermi mixture description to obtain the phase diagrams of Fermi-Fermi mixtures with equal or unequal masses and equal or unequal populations in the strong attraction limit. For this purpose, we analyzed first the exact boson-fermion and boson-boson scattering lengths as a function of mass anisotropy, and then we constructed the phase diagrams of Fermi-Fermi mixtures in the BEC regime.

We showed that three-dimensional nontrapped fermion mixtures with population imbalance exhibit phase separation in addition to the normal polarized mixture of fermions and uniform mixture of superfluid and excess fermions. In the BEC regime, we found two different nonuniform phase-separated states: PS(1), where there is phase separation between pure unpaired (excess) and pure paired fermions (molecular bosons); and PS(2), where there is phase separation between pure excess fermions and a mixture of excess fermions and molecular bosons. For equal mass mixtures, our results for the phase boundaries are quantitatively different from previous saddle-point results, and these quantitative differences become more pronounced for unequal mass mixtures when heavier fermions are in excess, indicating the importance of taking into account scattering processes beyond the Born approximation.

We also discussed the effects of trapping potentials on the density profiles of condensed and noncondensed molecular bosons, and excess fermions at zero and finite temperatures. At zero temperature, we found that almost all of the condensed bosons are at the center of the trap, while the excess fermions are pushed to the edges due to the repulsive boson-fermion interactions. At finite temperatures, we found that noncondensed pairs and excess fermions are created at the center of the trap at the expense of an overall reduction of condensed bosons. Finally, at temperatures above the BEC temperature, the number of condensed bosons vanish, and the system becomes a mixture of weakly interacting noncondensed bosons and excess fermions. Finally, we discussed that our findings can provide good quantitative comparisons to experiments performed in the same regime of validity of the theory (BEC regime), since the boson-fermion and boson-boson scattering parameters that enter our calculations are exact in the dilute limit.

Lastly, we think that it is important to perform experiments with Fermi-Fermi mixtures in the strong attraction limit (BEC regime) where the theoretical description is simple. In this limit, additional superfluid and normal phases and richer density profiles proposed here can be observed, and directly compared with the theory.

ACKNOWLEDGMENT

We thank National Science Foundation (DMR-0709584) for support.

[1] T. Bourdel, L. Khaykovich, J. Cubizolles, J. Zhang, F. Chevy, M. Teichmann, L. Tarruell, S. J. J. M. F. Kokkelmans, and C. Salomon, Phys. Rev. Lett. **93**, 050401 (2004).
[2] C. A. Regal, M. Greiner, and D. S. Jin, Phys. Rev. Lett. **92**, 040403 (2004).
[3] C. Chin, M. Bartenstein, A. Altmeyer, S. Riedl, S. Jochim, J. Hecker Denschlag, and R. Grimm, Science **305**, 1128 (2004).
[4] G. B. Partridge, K. E. Strecker, R. I. Kamar, M. W. Jack, and R. G. Hulet, Phys. Rev. Lett. **95**, 020404 (2005).
[5] J. Kinast, A. Turlapov, J. E. Thomas, Q. Chen, J. Stajic, and K. Levin, Science **307**, 1296 (2005).
[6] M. W. Zwierlein, J. R. Abo-Shaeer, A. Schirotzek, C. H. Schunck, and W. Ketterle, Nature (London) **435**, 1047 (2005).
[7] M. W. Zwierlein, A. Schirotzek, C. H. Schunck, and W. Ketterle, Science **311**, 492 (2006).
[8] G. B. Partridge, W. Lui, R. I. Kamar, Y. Liao, and R. G. Hulet, Science **311**, 503 (2006).
[9] Y. Shin, M. W. Zwierlein, C. H. Schunck, A. Schirotzek, and W. Ketterle, Phys. Rev. Lett. **97**, 030401 (2006).
[10] G. B. Partridge, W. Li, Y. A. Liao, R. G. Hulet, M. Haque, and H. T. C. Stoof, Phys. Rev. Lett. **97**, 190407 (2006).
[11] A. J. Leggett, in *Modern Trends in the Theory of Condensed Matter*, edited by A. Peralski and R. Przystawa (Springer-Verlag, Berlin, 1980).
[12] P. Nozières and S. Schmitt-Rink, J. Low Temp. Phys. **59**, 195 (1985).
[13] C. A. R. Sá de Melo, M. Randeria, and J. R. Engelbrecht, Phys. Rev. Lett. **71**, 3202 (1993).
[14] W. V. Liu and F. Wilczek, Phys. Rev. Lett. **90**, 047002 (2003).
[15] P. F. Bedaque, H. Caldas, and G. Rupak, Phys. Rev. Lett. **91**, 247002 (2003).
[16] A. Sedrakian, J. Mur-Petit, A. Polls, and H. Muther, Phys. Rev. A **72**, 013613 (2005).
[17] P. Castorina, M. Grasso, M. Oertel, M. Urban, and D. Zappala, Phys. Rev. A **72**, 025601 (2005).
[18] J. Carlson and S. Reddy, Phys. Rev. Lett. **95**, 060401 (2005).

[19] C. H. Pao, S.-T. Wu, and S. K. Yip, Phys. Rev. B **73**, 132506 (2006).
[20] D. E. Sheehy and L. Radzihovsky, Phys. Rev. Lett. **96**, 060401 (2006).
[21] J. Kinnunen, L. M. Jensen, and P. Torma, Phys. Rev. Lett. **96**, 110403 (2006).
[22] P. Pieri and G. C. Strinati, Phys. Rev. Lett. **96**, 150404 (2006).
[23] W. Yi and L. M. Duan, Phys. Rev. A **73**, 031604(R) (2006).
[24] T. N. De Silva and E. J. Mueller, Phys. Rev. A **73**, 051602(R) (2006).
[25] M. Haque and H. T. C. Stoof, Phys. Rev. A **74**, 011602(R) (2006).
[26] M. Iskin and C. A. R. Sá de Melo, Phys. Rev. Lett. **97**, 100404 (2006).
[27] C. Lobo, A. Recati, S. Giorgini, and S. Stringari, Phys. Rev. Lett. **97**, 200403 (2006).
[28] X.-J. Liu, H. Hu, and P. D. Drummond, Phys. Rev. A **75**, 023614 (2007).
[29] T. Mizushima, M. Ichioka, and K. Machida, e-print arXiv:cond-mat/07053361.
[30] M. Iskin and C. A. R. Sá de Melo, Phys. Rev. A **76**, 013601 (2007).
[31] E. Taylor, A. Griffin, and Y. Ohashi, Phys. Rev. A **76**, 023614 (2007).
[32] S. T. Wu, C. H. Pao, and S. K. Yip, Phys. Rev. B **74**, 224504 (2006).
[33] G.-D. Lin, W. Yi, and L.-M. Duan, Phys. Rev. A **74**, 031604(R) (2006).
[34] M. M. Parish, F. M. Marchetti, A. Lamacraft, and B. D. Simons, Phys. Rev. Lett. **98**, 160402 (2007).
[35] D. S. Petrov, C. Salomon, and G. V. Shlyapnikov, J. Phys. B **38**, S645 (2005).
[36] D. S. Petrov, Phys. Rev. A **67**, 010703(R) (2003).
[37] G. V. Skorniakov and K. A. Ter-Martisosian, Zh. Eksp. Teor. Fiz. **31**, 775 (1956) [Sov. Phys. JETP **4**, 648 (1957)].
[38] I. V. Brodsky, M. Yu. Kagan, A. V. Klaptsov, R. Combescot, and X. Leyronas, Phys. Rev. A **73**, 032724 (2006).
[39] J. Levinsen and V. Gurarie, Phys. Rev. A **73**, 053607 (2006).
[40] R. Grimm (private communication).
[41] T. Fukuhara, Y. Takasu, M. Kumakura, and Y. Takahashi, Phys. Rev. Lett. **98**, 030401 (2007).
[42] L. Viverit, C. J. Pethick, and H. Smith, Phys. Rev. A **61**, 053605 (2000).
[43] J. Tempere, M. Wouters, and J. T. Devreese, Phys. Rev. B **75**, 184526 (2007).
[44] M. Amoruso, A. Minguzzi, S. Stringari, M. P. Tosi, and L. Vichi, Eur. Phys. J. D **4**, 261 (1998).
[45] Y. Ohashi and A. Griffin, Phys. Rev. A **67**, 033603 (2003).
[46] A. Perali, P. Pieri, L. Pisani, and G. C. Strinati, Phys. Rev. Lett. **92**, 220404 (2004).